TITLE: Evolution in *Sinocyclocheilus* cavefish is marked by rate shifts, reversals and origin of novel traits

Ting-Ru Mao†,[1], Ye-Wei Liu†,[1], Madhava Meegaskumbura†,‡,[1,3], Jian Yang[2], Gajaba Ellepola[1,3], Gayani Senevirathne[4], Cheng-Hai Fu[1], Joshua B. Gross[5], Marcio R. Pie[6]

[1]Guangxi Key Laboratory for Forest Ecology and Conservation, College of Forestry, Guangxi University, Nanning, Guangxi, P.R.C.

[2]Key Laboratory of Environment Change and Resource Use, Beibu Gulf, Nanning Normal University, Nanning, Guangxi, P.R.C.

[3]Deparment of Molecular Biology and Biotechnology & Department of Zoology, Faculty of Science, University of Peradeniya, Peradeniya, Sri Lanka

[4]Department of Organismal Biology & Anatomy, University of Chicago, Chicago, IL, USA

[5]Department of Biological Sciences, University of Cincinnati, Cincinnati, Ohio, USA

[6]Departamento de Zoologia, Universidade Federal do Paraná, Curitiba, Paraná, Brazil 81531-980

† - equal contribution

‡ - corresponding author - madhava_m@mac.com

ABSTRACT

Epitomized by the well-studied *Astyanax mexicanus*, cavefishes provide important model organisms to understand adaptations in response to divergent natural selection. However, the spectacular *Sinocyclocheilus* diversification of China, the most diverse cavefish clade in the

world harboring nearly 75 species, demonstrate evolutionary convergence for many traits, yet remain poorly understood in terms of their morphological evolution. Here, using a broad sample of 49 species representative of this diversification, we analyze patterns of *Sinocylocheilus* evolution in a phylogenetic context. We categorized species into morphs based on eye-related condition: Blind, Micro-eyed (small-eyed), and Normal-eyed and we also considered three habitat types (Troglodytic – cave-restricted; Troglophilic – cave-associated; Surface – outside of caves). Geometric morphometric analyses show Normal-eyed morphs with fusiform shapes being segregated from Blind/Micro-eyed (Eye-regressed) morphs with deeper bodies along the first principal component ("PC") axis. The second PC axis accounts for shape complexity related to the presence of horns. Ancestral character reconstructions of morphs suggest at least three independent origins of Blind morphs, each with different levels of modification in relation to the typical morphology of ancestral Normal-eyed morphs. Interestingly, only some Blind or Micro-eyed morphs bear horns and they are restricted to a single clade (Clade B) and arising from a Troglodytic ancestral species. Our geophylogeny shows an east-to-west diversification spanning the Pliocene and the Pleistocene, with Troglodytic species dominating karstic subterranean habitats of the plains whereas predominantly Surface species inhabit streams and pools in hills to the west (perhaps due to the scarcity of caves). Integration of morphology, phylogeny and geography suggests *Sinocyclocheilus* are pre-adapted for cave dwelling. Analyses of evolutionary rates suggest that lineages leading to Blind morphs were characterized by significant rate shifts, such as a slowdown in body size evolution and a 3.3 to 12.5 fold increase in the evolutionary rate of eye regression. Furthermore, body size and eye size have undergone reversals, but horns have not, a trait that seem to require substantial evolutionary time to form. These results, compared to the *Astyanax* model system, indicate *Sinocyclocheilus* fishes

demonstrate extraordinary morphological diversity and variation, offering an invaluable model system to explore evolutionary novelty.

KEYWORDS: Phylomorphospace, Evolutionary Convergence, Blind fish, Troglodytism, Geophylogeny, Pre-adaptation

INTRODUCTION

Due to the absence of light, stable mean temperatures, absence of primary productivity, and paucity of dissolved oxygen, subterranean habitats are among the most challenging environments for life on earth (Ginet and Decou, 1977, Camacho, 1992). From surface-dwelling ancestral species, cavefish have secondarily adapted to live in cave systems, often demonstrating a remarkable array of morphological and behavioral adaptations (Soares and Niemiller, 2013; Yoshizawa, 2015). These involve enhanced sensation, and also dispensing of traits that incur a developmental or energetic cost. Cavefish species can be divided into two forms: troglophiles are closely associated with caves, but do not entirely depend on them, and troglobites are obligate cave dwellers (Dowling et al., 2002; Jingcheng and Weicheng, 2015). Troglobite fish *may* harbor special adaptations, such as complete eye loss, loss of pigmentation, changes in cranial symmetry, proliferation of neuromast sensory organs, development of horns, and in some species flat, hollow heads (Strecker et al., 2004; Zhao, 2006; Gross et al., 2008). Despite the ~200 cavefish species from across the world, large diversification of cavefishes is rare. However, one extensive diversification occurs in *Sinocyclocheilus*, a monophyletic group of cyprinid fishes endemic to China, which allows a robust analysis of trait evolution relative to troglomorphism in a phylogenetic context.

The specialized traits cavefish bear have led them to be developed as models of evolution especially with respect to adaptations to novel environments and evolutionary convergence (Culver et al., 1995; Dowling et al., 2002; Jeffery, 2001; Li et al. 2008; Strecker et al., 2004; Yang et al.， 2016). A lion's share of knowledge on evolution and development in cavefishes has come from *Astyanax mexicanus* (Mexican tetra), a species with both surface-dwelling (pigmented and eyed) and cave-dwelling morphs (depigmented and blind), which can readily interbreed (Borowsky, 2008). In contrast to this well-studied model system, *Sinocyclocheilus* species not only include blind and normal-eyed morphs (Lan et al., 2013), but demonstrate a continuum from blind to normal-eyed species. Indeed, members of the *Sinocyclocheilus* genus display remarkable morphological evolution with divergent cave-dwelling, cave-associated, and surface-dwelling species.

Sinocyclocheilus species are thought to have shared a common ancestor in the late Miocene, undergoing a spectacular diversification spanning the Pliocene and Pleistocene across the southwestern parts of China's 620,000 km^2 of karst habitats (Huang et al., 2008), with nearly 75 extant species (Jiang et al., 2019). This resulted in an adaptive diversification into subterranean refugia traversing the intersection of the Guizhou, Guangxi and Yunnan provinces around the time of the uplifting of Tibetan/Guizhou plateau (Li et al., 2008).

One of the most striking forms of cave adaptation in *Sinocyclocheilus* is variation in eye morphology, categorized often into three morphs (Zhao and Zhang, 2009), ranging from Normal-eyed to Micro-eyed (small-eyed) to Blind species. Of all Chinese hypogean fishes, 56 species show troglomorphism such as reduction and/or loss of eyes, pigmentation, and the gas bladder. Presence of a horn-like structure and hyper-development of the dorsal protuberance (similar to a humpback whale) are two additional unique characters to certain Chinese hypogean species

93 (Romero et al., 2009). These dramatic adaptations to cave life are reflected in the unique
94 morphology of these fish.

95 The morphology of *Sinocyclocheilus* is most likely attributed to their habitat and local
96 adaptations, however the precise function of certain morphologies (e.g., their horns and humps)
97 remains unknown (Ma and Zhao, 2012). For instance, many blind species are obligate cave
98 dwellers that have the ability to navigate along cave walls, cave-bottoms and within narrow
99 passages (Yoshizawa, 2015). Yet, others are open water species that navigate in the manner of
100 typical fish. There are also intermediate forms between these two principal morphs (Zhao and
101 Zhang, 2009). However, the morphology of these fishes is so extreme that substantial variation
102 in morphology is evident even within blind, intermediate and the open water species.

103 The pattern of body shape evolution in *Sinocyclocheilus* is a conundrum, which has not been
104 addressed in an evolutionary context. Here, we explore key patterns of morphological evolution
105 in these fishes, and demonstrate that the evolution in *Sinocyclocheilus* has been associated with
106 significant rate changes and trait reversals across their phylogenetic history.

107

108 **MATERIALS & METHODS**

109 *Phylogeny estimation*

110 We compiled sequence data from GenBank for two mtDNA fragments (*NADH4* and *cytb*) of
111 39 *Sinocyclocheilus* species, and the outgroup species *Linichthys laticeps* (Cyprinidae). In
112 addition, we generated sequence data for the *cytb* gene fragment of ten additional
113 *Sinocyclocheilus* species (Table S1). For these species, total genomic DNA was extracted using
114 the DNeasy Blood and Tissue Kit (Qiagen Inc., Valencia, CA) following the manufacturer's
115 protocols. DNA was amplified in 25-µL volume reactions: 3 mM $MgCl_2$, 0.4 mM of dNTP, 1X

116 buffer, 0.06 U of Taq DNA Polymerase, 2 mM of each primer. Thermocycling conditions
117 included an initial step at 94 °C for 3 min, followed by 35 cycles at 45 s at 94 °C, 1 min at 46-50
118 °C and 45 s at 48-56 °C, and a final step at 72 °C for 5 min. PCR products were electrophoresed
119 in a 1.5% agarose gel, stained with ethidium bromide and visualized under UV light.
120 Successfully amplified products were purified using MicroconTM Centrifugal Filter Units
121 (Millipore, Billerica, MA, U.S.A.). Sequencing reactions were carried out in 10 µl solutions
122 including the following final concentrations: 5 ng/µl of template DNA, 0.5 µl of Big DyeTM
123 (Applied Biosystems Inc., Foster City, CA, U.S.A.), 0.2 µM of each primer and 0.1X of reaction
124 buffer. The final product was purified using SephadexTM G-50 (GE Healthcare Bio-Sciences
125 AB, Uppsala, Sweden) for sequencing. Forward and reverse strands were reconciled using
126 Staden v.1.6.0 (Staden 1996). Sequences from both genes were concatenated and aligned
127 unambiguously using CLUSTALW (Thompson et al., 2003), as implemented in MEGA v. 6.0
128 (Tamura et al. 2013), for a total alignment length of 2155 bp. We used JMODELTEST v.2.1.10
129 (Santorum et al., 2014) to determine the best models of evolution for each fragment, which were
130 implemented in BEAST v.1.10.4 (Drummond and Rambaut, 2007) as a partitioned analysis to
131 estimate the phylogenetic relationships and relative divergence times within *Sinocyclocheilus*.
132 We calibrated the tree using the relative time period which diversification of *Sinocyclocheilus*
133 initiated around 11.31 Mya, a reference point obtained from (Chen et al., 2018). We used a strict
134 molecular clock and a calibrated Yule tree prior, as well as a GTR+I+G for each partition and
135 ran the analysis for 20 million generations using the Cipres Science Gateway Server (Miller et
136 al., 2010). Convergence was assessed by inspecting the log-output file in TRACER v.1.6
137 (Drummond et al., 2012), and by ensuring ESS values were above 200. The first 10% of the trees
138 were discarded, and the post burn-in trees were used to infer the maximum clade credibility tree

139 using TREEANNOTATOR v.1.4.4 (Rambaut and Drummond， 2019). The maximum clade
140 credibility tree, as well as a set of 1000 post burn-in topologies, were retained for further
141 analyses (see below).
142
143 *Morphometric data acquisition and analyses*
144 We assembled a database of images of referenced specimens of *Sinocyclocheilus* from
145 scaled photographs, which was complemented by species that we photographed (Table S2). The
146 final dataset included 90 images (54 from species descriptions and catalogues and 36 from
147 photographs by the authors) for 50 species, which included 70% of the total number of described
148 species for the genus. These images were used for geometric morphometrics analyses, which
149 were based on 15 landmarks (See Fig. 1A) and 180 sliding semi-landmarks, obtained using
150 tpsDig v. 2.16 (Rohlf, 2010). Semi-landmarks were collected as curves outlining the body. These
151 data were subsequently reduced to equidistant landmarks, and defined as semi-landmarks using
152 tpsUtil v. 1.46 (Rohlf, 2010). We then slid the landmarks using the bending energy method
153 (Gunz & Mitteroecker, 2013) implemented in GEOMORPH v.3.2.0 (Adams & Otárola-Castillo,
154 2013). The landmark coordinates were aligned using a generalized Procrustes superimposition
155 analysis (Adams *et al*., 2013), and a principal component analysis (PCA) was used to evaluate
156 shape variation within the sample.
157 Multiple images for the same species were used to obtain the landmarks and the mean of
158 their Procrustes coordinates were calculated to be used in later analyses. We also obtained
159 traditional linear measurements, namely standard length (SL), eye diameter (ED) and
160 standardized eye diameter (sED, calculated as the ratio between ED and SL).
161

Morphological and habitat evolution

Since shape variation in *Sinocyclocheilus* cavefishes occurs mostly in the anterior end of the fish and as one of the major features leading to this is eye-related, we considered the absence or the size of the eye (when present) as a proxy for the categorization of morphs. Since the eye size has an allometric association with body size, we used the standardized eye diameter (sED) in placing them into three morphological categories: Blind (eye absent); Micro-eyed (0.0 – 3.0mm); Normal-eyed (< 3.0mm) respectively. For ease of discussion, we considered Blind and Micro-eyed together as Regressed-eyed; Micro-eyed and Normal-eyed together as Eyed species.

Sinocyclocheilus were also categorized based on their habitat as Troglodytic, Troglophilic, and Surface species. Troglodytic species live in an obligatory association with caves, and are not sampled outside of caves. Caves, as meant here represent roofed-caves, submerged caves, and subterranean waterways that form windows intermittently with the surface. Troglophilic species live in a close association with caves and are sampled both in the vicinity of cave entrances and within caves. Finally, Surface species are found in habitats even when a cave is not found in close proximity and live in normal streams ponds and lakes as typical fish do, but they could venture into caves (underground water bodies) during unfavorable periods, when water is only available in caves. It should be noted here that this categorization is strictly habitat based and not morphology based (for instance, there are Normal-eyed species that are Troglodytic, Troglophilic or Surface). These habitat associations are based on published literature (Zhao and Zhang, 2009; Romero et al., 2009) and personal observations as outlined in Table S1.

To infer the number and timing of evolutionary shifts within eye-related morphs, horn distribution and the habitat type, we used stochastic character mapping (Nielsen, 2002; Huelsenbeck et al. 2003), as implemented in the make.simmap function in PHYTOOLS. On each of

185 the 1000 post burn-in trees obtained from BEAST, we used stochastic character mapping to
186 generate 100 potential histories. This approach therefore considers uncertainty both in the
187 evolutionary history of the traits as well as in the inferred topology of the phylogeny.

188 The landmark coordinates obtained were aligned using a generalized Procrustes
189 superimposition analysis (Adams et al., 2013), and a principal component analysis (PCA) was
190 used to explore shape variation within the sample. In addition, we described the eye-related
191 morphological variation in *Sinocyclocheilus* by estimating ancestral states of SL and ED and
192 visualizing them using traitgrams (Evans et al., 2009) as implemented in the phenogram function
193 in PHYTOOLS 0.7.20 (Revell, 2012) using the maximum clade credibility tree. We also visualized
194 the evolution of both traits simultaneously using a phylomorphospace (a projection of the tree
195 into morphospace, *sensu* Sidlauskas, 2008) using the phylomorphospace function in PHYTOOLS.

196

197 *Evolutionary rate variation in eye related morphs*

198 We tested whether the evolutionary rates of the studied continuous traits (SL, ED, sED) are
199 significantly different in different morphs. We used 100 potential trait histories from stochastic
200 character mapping and then fit two alternative models of evolution on each studied trait, one that
201 fixes the rate of evolution to be identical between morphs against an alternative model in which
202 the morphs have separate rates. We calculated the Akaike Information Criterion for small sample
203 size (AICc) from the maximum likelihood estimate on each tree using the brownie.lite function
204 in PHYTOOLS. Finally, if a multi-rate model provided a better fit to the data, we calculated model-
205 averaged estimates of evolutionary rates for each morph. Unless otherwise indicated, all analyses
206 were conducted using R v. 3.6.0 (R Core Team, 2019).

207

208 *Geophylogeny analyses*

209 We could not carry out a formal biogeographical analysis, given that their high endemism
210 and the complex pattern of underground connections between caves limits the establishment of
211 reasonable biogeographical areas. However, we assessed the geographical structuring
212 of *Sinocyclocheilus* diversification by building a geophylogeny on GenGIS v. 2.5.3 (Parks et al.,
213 2013) based on the maximum credibility tree.

214

215 **RESULTS**

216 The maximum credibility tree of *Sinocyclocheilus* is shown in Fig. 2 together with the
217 reconstruction of ancestral states for eye-related morphs; we consider four major clades
218 (A,B,C,D), as previously reported by other authors (Zhao and Zhang, 2009). Despite the inherent
219 uncertainty in ancestral state reconstructions, it is clear that Blind species evolved at least three
220 times in *Sinocyclocheilus*. Two of these events involved single species evolving from Normal-
221 eyed ancestors, namely *S. xunlensis* and *S. anophthalmus*. On the other hand, the third lineage of
222 blind *Sinocyclocheilus,* Clade B, includes several closely related species of Blind, Micro-eyed
223 and a few Normal-eyed species, with two cases of reversal from either Micro-eyed or Blind to
224 Normal-eyed morphs, namely *S. zhenfengensis* and *S. brevibarbatus* (Fig. 2. All four clades
225 contain Regressed-eyed species and comparatively, clade Blind contains the most cases.
226 Interestingly, clade B originated around the time of the beginning of the aridification process in
227 China in the late Pliocene, whereas the other two transitions to blind species were much more
228 recent (Fig. 2.

229 Interestingly, the evolution of body size and eye diameter seem to have often involved
230 reversals, with little correspondence between body size (Fig. 3A) or eye diameter (Fig. 3B) and

231 their corresponding morphs, except for the case of blind species for which eye diameter is
232 necessarily zero. On the other hand, morphs are clearly distinguished when eye diameter and
233 body size are visualized simultaneously (Fig. 3C), which suggests that the evolution of different
234 morphs is achieved by altering the relationships between body size and eye diameter. Habitat
235 associations traced on the phylomorphospace (Fig. 3D) indicates that species with regressed eyes
236 and small-to-medium body sizes are obligate cave dwellers. However, normal eyed species can
237 be Troglodytic, Troglophilic or surface dwellers regardless of their body size. Interestingly all
238 horned species are obligate cave dwellers while all cave species are not horned (Fig. 3E).

239 A more precise description of the overall changes associated with different morphs can be
240 visualized in the projections build from the geometric morphometrics analyses (Fig. 1B). The
241 first PC, which accounted for approximately 32% of the variance in the dataset (see Table S3),
242 tended to distinguish the slender Normal-eyed species on the left and Micro/Blind species on the
243 right, which were characterized by changes in shape and widening of the anterior dorsal area
244 between mouth and beginning of the dorsal fin of their body, resulting in a shift from the
245 fusiform shape of the Normal-eyed forms to a more "boxy" form of the Micro-eyed and Blind
246 forms. The second PC, which explained approximately 17% of the variance in the dataset,
247 emphasized the differences in the type of dorsoventral broadening of the mid-section between
248 morphs, with a shortening of the tail region (Fig. 1B). The variation in this axis is very high
249 among the Micro-eyed and Blind forms when compared to the Normal morphs.

250 The multiple-rate model of evolution provided the best fit to the data for all three
251 quantitative traits (ΔAIC=2.7, 10.7 and 7.9 respectively for ED, sED and SL; Table 1), indicating
252 that the evolution of different *Sinocyclocheilus* morphs was associated with significant changes
253 in their evolutionary rates. However, there were intriguing differences between traits in their

254 rates (Table 2). The rates of evolution of eye diameter and standardized eye diameter were
255 similar between Normal-eyed and Micro-Eyed species, but increased between 3.3 to 12.56 times
256 during shifts towards Blind species.

257 Geophylogeny represents the phylogeny overlaid across the geographic location of each
258 species, where phylogenetic clustering is evident across the landscape. Considering the
259 distribution of *Sinocyclocheilus,* we mainly see a pattern where the basal, Normal-eyed morphs
260 are placed in the east, a substantial portion of Blind/Micro-eyed (Regressed-eyed) species are in
261 the center, and Normal-eyed morphs are predominant towards the western mountains (Fig. 4).

262

263 **DISCUSSION**

264 ***Habitat utilization in context of eye-morphology***

265 Integrating evolution of eye size and habitat manifests interesting and previously
266 unrecognized evolutionary patterns in the evolution of *Sinocyclocheilus*. The Eye-size based
267 ancestral reconstruction suggests the base of the phylogeny is most likely an Eyed species (i.e.
268 Normal- or Micro-), but habitat reconstructions places, with high probability, Troglodytic species
269 at the base (Fig. S1). This suggests an ancestral Eyed-species evolved a Troglodytic habit before
270 they became blind. This may be an example of preadaptation in *Sinocyclocheilus*, i.e., the
271 advancement of a functional change with little or no evolutionary modification (Ardila, 2016). In
272 *Astyanax* cavefish, surface-dwelling forms are scotophilic, they prefer to remain away from
273 direct light suggesting that scotophilia may be preadaptive for colonizing the dark, cave
274 environment (Espinasa et al., 2001). In *Sinocyclocheilus*, since a basal (eyed) species
275 demonstrated preference for the cave habitat, this preadaptation to darkness may hint towards
276 why certain species tend to become cave-dwellers while others do not. This pattern is supported

277 by two principal lines of evidence. First, most of the basal species are eyed, and Troglodytic
278 (except for one species with an unusual eye-related polymorphic condition that we discuss
279 below). Second, the most westward group (Clade D; Normal-eyed Surface fish), re-colonized
280 caves whenever cave habitats were available within that area, suggesting a strong predisposition
281 for cave-dwelling across all *Sinocyclocheilus*. In other words, when caves were present,
282 members of *Sinocylocheilus,* irrespective of eye-related condition, preferred the cave habitat.

283 The preference for caves may not be a preference for darkness, but in fact a preference for
284 depth, in search of water for survival. In a karstic environment where drying of surface running
285 water is common, a preference for such deeper habitats may have provided an evolutionary
286 advantage. In the presence of an array of subterranean waterways, such a predisposition would
287 have given rise to the eye-regressed forms living close to, or associated with, caves that are
288 characteristic of the genus.

289 Furthermore, apart from the Troglodytic and Troglophilic species of Clade D, some of the
290 putative Surface species of Clade D are often observed at the entrances of caves or at windows to
291 subterranean rivers (Zhao and Zhang, 2009). Hence, with more intensive ecological studies,
292 some species recognized as Surface species may indeed be Troglophilic species, bolstering the
293 notion that *Sinocyclochelus* are predisposed to seek deeper waters of the karstic caves.

294 Resource utilization plays a key survival role in harsh environments (Culver and Pipan,
295 2009). Some of the Troglophilic, eyed-species are nocturnal, emerging from submerged caves,
296 presumably to feed at night to reduce competition from other non-cave inhabiting fish species
297 (personal observations). Some species like *S. altishoulderus, S. donglanensis* (Romero et al.,
298 2009), *S. bamaensis* (Su et al., 2003), *S. malacopterus* (Chen et al., 2017) and *S. longibarbatus*
299 (personal observation, video evidence as Supplementary information); are known to come out of

300 caves during the high water season, presumably to feed and breed. This explains dependence on
301 the cave as a diurnal refugium, from where these species can exploit the surface habitats at night.
302 Strategies such as this, where multiple resources are utilized simultaneously, points to the
303 adaptability of some *Sinocyclocheilus* species, resulting in their evolutionary success in a harsh
304 and changing environment. Hence, the cave entrances are possibly an important ecotone that is
305 important in *Sinocyclochelius* diversification and conservation.

306 Season and time of day seem to be important factors in determining habitat utilization
307 patterns, but this level of resolution in habitat data is not currently available for a majority of the
308 species to carry out a comprehensive habitat analysis across the diversification – indeed, many
309 species are known only from one or a few specimens (Zhao and Zhang, 2009).

310

311 ***Adaptations in the light of geophylogeny***

312 In combination with the data analyzed, basal *Sinocyclocheilus* (Clade A) are Normal-Eyed,
313 predominantly cave dwelling and non-horned species from the Eastern region of their
314 distribution. As pointed out, this suggests that the earliest ancestors of *Sinocyclocheilus* species
315 where Normal-eyed and but still lived in close association with caves. The ancestral
316 reconstructions suggest that the affinity to caves would have evolved early and is present in most
317 *Sinocyclocheilus.* The clade comprising basal species are from the east of the *Sinocyclocheilus*
318 distribution, i.e. the He Jiang and Gui Jiang river basin in northeastern Guangxi, and hence, it
319 seems that the diversification of these fish occurred from East to West (Fig. 4).

320 Within this predominantly Normal-eyed clade (Clade A), there is an exception,
321 *Sinocyclocheilus guanyangensis*, a species that we coded as Micro-eyed, has Normal-Eyed,
322 Micro-eyed and effectively Blind morphs within the same population – polymorphic for this

323 trait. But these blind morphs have their eyes completely covered by skin and the Micro-eye is not
324 itself degenerate. This kind of condition has been noted in several other taxa also (*S. xunlensis*
325 and *S. flexuodorsalis* – not available for our analysis), but is uncommon. This suggests a degree
326 of polymorphism for this trait, suggesting that the earliest ancestors of *Sinocyclocheilus* may
327 have been able to lose or gain eyes relatively easily as an adaptation to local conditions, this
328 ability appears several times within this cave-driven diversification.

329 The major adaptation for cave dwelling evolves predominantly in the expansive karstic area
330 in northwestern Guangxi (associated with the Liu Jiang basin and Hongshui river basin joining
331 the main Xijiang River system from the North), in Clade B, the southeastern corner of Guizhou
332 province (upper reaches of Hongshui River) and the northeastern plateau of Yunnan province.
333 This region can be considered the center for novel adaptations for *Sinocyclocheilus,* where these
334 fishes express their full morphological diversity, blindness, micro-eyedness, and their remarkable
335 horns. In the shape-related analyses, these species cluster on the right of morphospace (Fig. 1B).
336 The deeper caves and extensive subterranean river system associated with the Guangxi plains
337 (Zhao and Zhang, 2009) would have facilitated this extensive adaptive diversification (Fig. 4).

338 The karstic northwestern region that the Guangxi-dominated Clade (Clade B) experiences
339 drought conditions during much of the year, and one of the major sources of rain for the region is
340 through storms sweeping from the southeast that are strong enough to persist through the vast
341 plains of Guangxi, mainly from April to August (Zhao and Zhan, 2009). During unfavorable
342 periods, these fishes seem to have found refuge in the subterranean caves. The morphologically
343 most diverse clade being present in the region where the climatic conditions are most
344 unfavorable for surface fish, reinforces the notion that *Sinocyclocheilus* species adapted to life in
345 caves as climatic refuges (Zhao and Zhang, 2009).

346 The distribution of Clade C, characterized by mostly Normal-eyed but Troglodytic species
347 largely overlaps Clade B. In Clade C, the single Blind species (*S. xunlensis*) and the two Micro-
348 Eyed species (*S. cyphotergous* and *S. multipunctatus*) are shown within a narrow geographic area
349 on the Liu Jiang and Hongshui river system (Fig. 4).

350 Species in the clade that is found in the west (Clade D), predominantly on the hilly terrain of
351 Yunnan plateau, are predominantly Normal-eyed Surface species lacking horns (Fig. 1, Fig. 4).
352 However, wherever there are cave habitats and subterranean river systems, some of these
353 putative surface species have become facultative or obligate cave species. The obligate cave
354 species found within the region, *S. anophthalmus*, is blind. However, this Blind species stands
355 clustered with the Normal-eyed morphs in the morphospace, signifying that the shape of the
356 species has not extensively changed, possibly due to recent (Pleistocene) invasion of the cave
357 habitat from a Normal-eyed ancestor (Fig. 2) – time since becoming blind is not been long
358 enough for change into the box-like shape of the Blind species of Clade B.

359 Horn distributions show several peculiar trends. In most *Sinocyclocheilus* species, a
360 prominent hump is present (He et al., 2013). However, this hump is markedly low in the Normal-
361 eyed surface inhabiting species of the Yunnan clade (Fig. 4). For the species that bears a horn,
362 the horn represents the region in which the dorso-frontal hump is present, and always occurs
363 before the hump begins, at the boundary of the edge of the dorsal skull. The exception to this is
364 *S. cyphotergous* (Clade C), where a horn like structure is placed on top of the hump. *S.*
365 *cyphotergous,* a species found in clade C, is phylogenetically separate from other horned species,
366 suggesting that the origins of the "horn" for this species is evolutionarily different from the other
367 horned species (Fig. S2). Though the function of the horn remains unknown (protection of head,
368 anchoring in strong current and protection of head has been suggested; Zhao and Zhang, 2009),

369 functionally this structure may be similar to other species, if it is actually anchoring in strong
370 current is the main function.

371 The rates of evolution of various traits show some incongruent (non-allometric), but
372 interesting patterns that can be explained in the context to adaptations to a Troglodytic condition.
373 The rates of evolution in eye diameter are similar between Normal- and Micro-Eyed species but,
374 increases dramatically (3.3-12.56 times) with shifts towards blind forms. However, body size
375 evolution for these morpho groups shows a reversed pattern, with a 0.03 decrease in body size
376 evolution in the Blind morphs compared to the eyed-morphs. These patterns in rate variation
377 suggest that the evolution of Blind morphs to a Troglodytic habitat were simultaneously
378 associated with an increase in the rate of evolution of the eye-size degeneration and a decrease in
379 the rate of body size evolution. The smaller body size resulting from a sluggish rate of change
380 will facilitate both navigation within constricted spaces and sustenance on a limited supply of
381 resources expected to be experienced in subterranean habitats.

382 Much of our collective knowledge of the patterns and mechanisms of regressive evolution
383 come from studies of animals that have colonized the subterranean biome. Within this group, a
384 several studies have focused on the Mexican tetra, *Astyanax mexicanus* (Jeffery, 2009). This
385 natural animal model system comprises multiple cave-adapted morphs and a surface-dwelling
386 morph that resides in near the caves themselves (Gross, 2012). Since the discovery of *Astyanax*
387 cavefish in 1936, countless studies have provided insight to the developmental and genetic bases
388 for cave-associated traits (Hubbs and Innes, 1936). Indeed, much of this insight has emerged
389 from the interbreeding studies of conspecific cave and surface morphs (reviewed in Wilkens,
390 2016). However, several aspects of regressive evolution and troglomorphic adaptation remain
391 unresolved. Owing to several of the differences with *Astyanax*, we argue that *Sinocyclocheilus* is

392 well-positioned to provide important new insights to broader patterns of diversification and
393 adaptation in cave-dwelling organisms.

394 For instance, *Astyanax* represents a single species with 30 different interfertile populations
395 from a relatively small geographic location (Wilkens and Strecker, 2017). In contrast,
396 *Sinocyclochelius* harbors about 75 species (49 in our study) inhabiting diverse geographic
397 biomes across a much larger geographic area. Moreover, while *Astyanax* cavefish converge on
398 similar phenotypes (regressed vision and pigmentation), they are not regarded as having
399 numerous morphological novelties. In contrast, *Sinocyclocheilus* species have recurrently
400 evolved a unique "horn" (Soares et al., 2019) from several eyeless species. Similarly, the larger
401 number of *Sinocyclocheilus* species allows keener resolution for understanding broad
402 phylogenetic processes, such as trait reversals and directions of diversification. Although a
403 reversal from an eyeless to an eyed form has been reported for one cave population in *Astyanax*
404 (Caballo Moro; Krishnan and Rohner, 2017), this phenomenon appears to be much less common
405 than in *Sinocyclocheilus*. Additionally, a clear polarity of diversification is lacking in *Astyanax*
406 cavefish, rather ancient stocks of surface-dwelling forms appear to have recurrently invaded
407 caves to the east (i.e., Sierra de El Abra caves), with more recent invasions having occurred in
408 the northern (Sierra de Colmena) and the western caves (Sierra de Guatemala; Bradic et al.,
409 2012). However, the well-characterized gene flow between the cave and surface waters obscures
410 the ability to understand clear boundaries between different cave groups. Further, most *Astyanax*
411 cave populations are believed to have diverged over the course of the last ~200 – 500 Ky
412 (Herman et al., 2018). By contrast, *Sinocyclocheilus* species are much older, and therefore one
413 can determine how longer-term processes unfold in these cave-dwelling animals. Thus, despite
414 clear phylogenetic differences between *Astyanax* and *Sinocyclocheilus*, both genera have the

ability to provide complementary and critical insights to the processes underlying cave evolution and diversification.

The integration of morphology, phylogeny, rate analyses, dating and distribution show not only several remarkable patterns of evolution, but also interesting exceptions to these patterns that signifies the diversification of *Sinocyclocheilus* as a unique model system to study evolutionary novelty.

ACKNOWLEDGEMENTS

We thank the following institutions and individuals: funding from Guangxi University Special Talent Recruitment Grant to MM; funding from National Natural Science Foundation of China (31860600 and Guangxi Natural Science Foundation (2017GXNSFFA198010) JY; Shipeng Zhou, Bing Chen, Dan Sun, Jayampathi Herath and Amrapali Rajput for assistance in the field; Ethical review approval from Guangxi University.

REFERENCES

Adams, D. C., and E. Otárola-Castillo. 2013. geomorph: an r package for the collection and analysis of geometric morphometric shape data. Methods Ecol Evol 4:393–399.

Adams, D. C., F. J. Rohlf, and D. E. Slice. 2013. A field comes of age: geometric morphometrics in the 21st century. Hystrix, the Italian Journal of Mammalogy 24:7–14.

Ardila, A. 2016. The Evolutionary Concept of “Preadaptation” Applied to Cognitive Neurosciences. Front. Neurosci. 10:103.

Borowsky, R. 2008. Breeding *Astyanax mexicanus* through Natural Spawning. Cold Spring Harbor Protocols 2008:pdb.prot5091-pdb.prot5091.

438 Bradic, M., P. Beerli, F. J. García-de León, S. Esquivel-Bobadilla, and R. L. Borowsky. 2012.
439 Gene flow and population structure in the Mexican blind cavefish complex (*Astyanax*
440 *mexicanus*). BMC Evol Biol 12:9.
441 Camacho , A. I. ed. 1992. The Natural History of Biospeology. Monographs of the National
442 Museum of Natural Sciences. . National Museum of Natural Sciences., Madrid.
443 Chen, Y.-Y., R. Li, C.-Q. Li, W.-X. Li, H.-F. Yang, H. Xiao, and S.-Y. Chen. 2018. Testing the
444 validity of two putative sympatric species from *Sinocyclocheilus* (Cypriniformes:
445 Cyprinidae) based on mitochondrial cytochrome b sequences. Zootaxa 4476:130.
446 Chen, Z. M., J. Luo, H. Xiao, and J. X. Yang. 2010. Subterranian fishes of China. Pp. 397–
447 414 *in* Biology of Subterranean Fishes. E. Trajano, M. E. Bichuette, B.G. Kapoor (eds）.
448 Science Publishers, USA.
449 Culver, D. C., T. C. Kane, and D. W. Fong. 1995. Adaptation and natural selection in caves: the
450 evolution of Gammarus minus. Harvard University Press, Cambridge, Mass.
451 Culver, D. C., and T. Pipan. 2009. The biology of caves and other subterranean habitats. Oxford
452 University Press, New York.
453 Dowling, T. E., D. P. Martasian, and W. R. Jeffery. 2002. Evidence for Multiple Genetic Forms
454 with Similar Eyeless Phenotypes in the Blind Cavefish, *Astyanax mexicanus*. Molecular
455 Biology and Evolution 19:446–455.
456 Drummond, A. J., and A. Rambaut. 2007. BEAST: Bayesian evolutionary analysis by sampling
457 trees. BMC Evol Biol 7:214.
458 Drummond, A. J., M. A. Suchard, D. Xie, and A. Rambaut. 2012. Bayesian Phylogenetics with
459 BEAUti and the BEAST 1.7. Molecular Biology and Evolution 29:1969–1973.

460 Espinasa, L., P. Rivas-Manzano, and H. E. Pérez. 2001. A New Blind Cave Fish Population of
461 Genus *Astyanax*: Geography, Morphology and Behavior. Environmental Biology of Fishes
462 62:339–344.
463 Evans, M. E. K., S. A. Smith, R. S. Flynn, and M. J. Donoghue. 2009. Climate, Niche Evolution,
464 and Diversification of the "Bird-Cage" Evening Primroses (*Oenothera* , Sections *Anogra*
465 and *Kleinia*). The American Naturalist 173:225–240.
466 Ginet, R., and V. Decu. 1977. Initiation à la biologie et à l'écologie souterraines. J.-P. Delarge,
467 Paris.
468 Gross, J. B. 2012. The complex origin of *Astyanax* cavefish. BMC Evol Biol 12:105.
469 Gross, J. B., M. Protas, M. Conrad, P. E. Scheid, O. Vidal, W. R. Jeffery, R. Borowsky, and C. J.
470 Tabin. 2008. Synteny and candidate gene prediction using an anchored linkage map of
471 *Astyanax mexicanus*. Proceedings of the National Academy of Sciences 105:20106–20111.
472 Gunz, P., and P. Mitteroecker. 2013. Semilandmarks: a method for quantifying curves and
473 surfaces. Hystrix, the Italian Journal of Mammalogy 24(1):103-109.
474 He, Y., X. Y. Chen, T. Q. Xiao, and J. X. Yang. 2013. Three-dimensional morphology of the
475 *Sinocyclocheilus hyalinus* (Cypriniformes: Cyprinidae) horn based on synchrotron X-ray
476 microtomography . Zoological Research 34(4−5):128–134.
477 Herman, A., Y. Brandvain, J. Weagley, W. R. Jeffery, A. C. Keene, T. J. Y. Kono, H. Bilandžija,
478 R. Borowsky, L. Espinasa, K. O'Quin, C. P. Ornelas-García, M. Yoshizawa, B. Carlson, E.
479 Maldonado, J. B. Gross, R. A. Cartwright, N. Rohner, W. C. Warren, and S. E. McGaugh.
480 2018. The role of gene flow in rapid and repeated evolution of cave-related traits in Mexican
481 tetra, *Astyanax mexicanus*. Mol Ecol 27:4397–4416.

482 Huang, Q., Y. Cai, and X. Xing. 2008. Rocky Desertification, Antidesertification, and
483 Sustainable Development in the Karst Mountain Region of Southwest China. AMBIO: A
484 Journal of the Human Environment 37:390–392.
485 Hubbs, C. L., and W. T. Innes . 1936. The first known blind fish of the family Characidae: A
486 new genus from Mexico. Occasional papers of the Museum of Zoology, University of
487 Michigan 342:1–10.
488 Huelsenbeck, J. P., R. Nielsen, and J. P. Bollback. 2003. Stochastic Mapping of Morphological
489 Characters. Systematic Biology 52:131–158.
490 Jeffery, W. R. 2001. Cavefish as a Model System in Evolutionary Developmental Biology.
491 Developmental Biology 231:1–12.
492 Jeffery, W. R. 2009. Regressive evolution in *Astyanax* cavefish. Annual Review of Genetics
493 43:25–47.
494 Jiang, W. S., J. Li, X. Z. Lei, Z. R. Wen, Y. Z. Han, J. X. Yang, and J. B. Chang. 2019.
495 *Sinocyclocheilus sanxiaensis*, a new blind fish from the Three Gorges of Yangtze River
496 provides insights into speciation of Chinese cavefish. Zoological research 40(6):552–557.
497 Jingcheng, R., and Y. Weicheng. 2015. A Review of Progress in Chinese Troglofauna Research.
498 Journal of Resources and Ecology 6:237–246.
499 Krishnan, J., and N. Rohner. 2017. Cavefish and the basis for eye loss. Phil. Trans. R. Soc. B
500 372:20150487.
501 Lan, J. H., X. Gan, T. J. Wu, and J. Yang. 2013. Cave fishes of Guangxi, China. Science Press,
502 Beijing.
503 Li, Z., B. Guo, J. Li, S. He, and Y. Chen. 2008. Bayesian mixed models and divergence time
504 estimation of Chinese cavefishes (Cyprinidae: *Sinocyclocheilus*). Sci. Bull. 53:2342–2352.

505 Lunghi, E., Y. Zhao, X. Sun, and Y. Zhao. 2019. Morphometrics of eight Chinese cavefish
506 species. Sci Data 6:233.
507 Ma, L. and Y.H. Zhao. 2012. Cavefish of China. in: White, W.B.; and D.C. Cuvier, editors.
508 Encyclopedia of Caves. Pp. 107—125 Elsevier. ISBN 9780123838322
509 Miller, M. A., W. Pfeiffer, and T. Schwartz. 2010. Creating the CIPRES Science Gateway for
510 inference of large phylogenetic trees. Pp. 1–8 *in*. New Orleans, LA.
511 Nielsen, R. 2002. Mapping Mutations on Phylogenies. Systematic Biology 51:729–739.
512 Parks, D. H., T. Mankowski, S. Zangooei, M. S. Porter, D. G. Armanini, D. J. Baird, M. G. I.
513 Langille, and R. G. Beiko. 2013. GenGIS 2: Geospatial Analysis of Traditional and Genetic
514 Biodiversity, with New Gradient Algorithms and an Extensible Plugin Framework. PLoS
515 ONE 8:e69885.
516 R Development Core Team. 2019. a language and environment for statistical computing:
517 reference index. R Foundation for Statistical Computing, Vienna.
518 Rambaut, A., and A. J. Drummond. 2013. TreeAnnotator v1.10.4. Available as part of the
519 BEAST package at http://beast.bio.ed.ac.uk. .
520 Revell, L. J. 2012. phytools: an R package for phylogenetic comparative biology (and other
521 things): phytools: R package. Methods in Ecology and Evolution 3:217–223.
522 Rohlf, F. J. 2010. tpsDig 2.16 edn. at http://life.bio.sunysb.edu/morph/.
523 Romero, A., Y. Zhao, and X. Chen. 2009. The Hypogean fishes of China. Environ Biol Fish
524 86:211–278.
525 Santorum, J. M., D. Darriba, G. L. Taboada, and D. Posada. 2014. jmodeltest.org: selection of
526 nucleotide substitution models on the cloud. Bioinformatics 30:1310–1311.

527 Sidlauskas, B. 2008. Continuous and arrested morphological diversification in sister clades of
528 characiform fishes: A phylomorphospace approach. Evolution 62:3135–3156.
529 Soares, D., and M. L. Niemiller. 2013. Sensory Adaptations of Fishes to Subterranean
530 Environments. BioScience 63:274–283.
531 Soares, D., M. Pluviose, and Y. Zhao. 2019. Ontogenetic development of the horn and hump of
532 the Chinese cavefish *Sinocyclocheilus furcodorsalis* (Cypriniformes: Cyprinidae). Environ
533 Biol Fish 102:741–746.
534 Staden, R. 1996. The staden sequence analysis package. Mol Biotechnol 5:233–241.
535 Strecker, U., V. H. Faúndez, and H. Wilkens. 2004. Phylogeography of surface and cave
536 *Astyanax* (Teleostei) from Central and North America based on cytochrome b sequence data.
537 Molecular Phylogenetics and Evolution 33:469–481.
538 Su, R., J. Yang, and G. Cui. 2003. Taxonomic review of the genus *Sinocrossocheilus wu*
539 (Teleostei: Cyprinidae), with a description of four new species. Zoological Studies 42:420–
540 430.
541 Tamura, K., G. Stecher, D. Peterson, A. Filipski, and S. Kumar. 2013. MEGA6: Molecular
542 Evolutionary Genetics Analysis Version 6.0. Molecular Biology and Evolution 30:2725–2729.
543 Thompson, J. D., T. J. Gibson, and D. G. Higgins. 2003. Multiple Sequence Alignment Using
544 ClustalW and ClustalX. Current Protocols in Bioinformatics 00: 2.3.1-2.3.22.
545 Wilkens, H. 2016. Genetics and hybridization in surface and cave *Astyanax* (Teleostei): a
546 comparison of regressive and constructive traits. Biol. J. Linn. Soc. 118:911–928.
547 Wilkens, H., and U. Strecker. 2017. Surface and cave populations of Mexican *Astyanax*. Pp. 37–
548 52 *in* Evolution in the Dark . Springer, Berlin, Heidelberg.

549 Yang, J., X. Chen, J. Bai, D. Fang, Y. Qiu, W. Jiang, H. Yuan, C. Bian, J. Lu, S. He, X. Pan, Y.
550 Zhang, X. Wang, X. You, Y. Wang, Y. Sun, D. Mao, Y. Liu, G. Fan, H. Zhang, X. Chen, X.
551 Zhang, L. Zheng, J. Wang, and L. Cheng. 2016. The *Sinocyclocheilus* cavefish genome
552 provides insights into cave adaptation. BMC Biology 14:1.
553 Yoshizawa, M. 2015. Behaviors of cavefish offer insight into developmental evolution: Evo-
554 Devo of cave fish behaviour. Mol. Reprod. Dev. 82:268–280.
555 Zhao, Y. 2006. Cavefishes: concept, diversity and research progress. Biodiversity Science
556 14:451.
557 Zhao, Y., and C. Zhang. 2009. Endemic Fishes of *Sinocyclocheilus* (Cypriniformes: Cyprinidae)
558 in China -Species diversity, cave adaptation, systematics and zoogeography. Science Press,
559 Beijing.
560

Main Figures

Fig. 1. (A) A specimen of *Sinocyclocheilus altishoulderus* indicating the position of 15 landmarks (red: larger points indicated by numbers 1-15) and 180 semi-landmarks (red: smaller point) used for the calculation of Procrustes coordinates and traditional linear measurements (SL: standard Length, ED: eye diameter and sED: standardized eye diameter) used in the geometric morphometric analyses. (B) **PCA showing the variation in body shape of the genus *Sinocyclocheilus* traced with eye morphology and habitat occupation.** PC1 and PC2 accounts for 32% and 17% of the variance respectively. A shift from the fusiform shape of the Normal-eyed surface forms to a more "boxy" form of the Micro-eyed and Blind forms is evident.

Fig. 2. Ancestral state reconstruction of morphology (Blind, Mico-eyed & Normal-eyed) on a time calibrated phylogeny. Posterior probabilities of node support also shown on the tree. **Maximum-likelihood reconstructions for the ancestral state of the eye-trait morphology (Blind, Micro and Normal-eyed morphs) on a time calibrated phylogeny.** A, B, C and D are four major clades. Posterior probabilities of node support values of 100% are indicated by *. Key events of *Sinocyclocheilus* evolution includes; at least three independent evolutionary events for Blind morphs; Blind, Micro-eyed and a few Normal-eyed species in clade B, with two cases of reversal from either Micro-eyed or Blind to Normal-eyed species.

Fig. 3. **Temporal patterns of body size and eye diameter in *Sinocyclocheilus* from the perspective of their eye trait related morphs.** The traitgrams suggests that the evolution of different morphs is attained by altering the allometric relationships between body size and eye

584 diameter. A. Traitgram of body size ; B. traitgram of eye size; C. Eye related morphs traced on
585 the phylomorphospace indicating clear separation of the three morphs in the morphospace.
586 (D)Habitat associations traced on the phylomorphospace showing species having eye diameter
587 <3mm and small to medium body sizes are obligate cave dwellers whereas species with eye
588 diameter >3mm can be Troglodytic, Troglophilic or Surface dwellers regardless of their body
589 size (E) Horn related morphs traced on the phylomorphospace indicating the presence of a horn
590 in smaller fish with reduced eye size. Horned species are Troglodytes.
591
592 **Fig. 4. Geophylogeny, the phylogeny laid across the geographic distribution of the species**
593 **considered in the analysis, with eye-related morphology, habitats, and horn-existence of the**
594 **species traced**. A pattern where basal, Normal-eyed, Troglodytic species are placed in the east,
595 predominantly Blind/Micro-eyed/Normal-Eyed, Troglodytic species in the center and Normal-
596 eyed, Surface dwelling species towards the western mountains is evident, indicating an East to
597 west dispersion of the genus *Sinocyclocheilus* across South and South Western China. Eye
598 specializations mostly occurred in Clade B, and horn evolution occurred exclusively in Clade B,
599 within the Central range of the *Sinocyclocheilus* distribution.
600
601

602 ## Main Tables:

603 **Table 1. Model fit and estimated Brownian rate parameters for three traits (ED, sED and**

604 **SL) in eye related morphs of *Sinocyclocheilus*.** Multiple-rate models of evolution providing the

605 best fit to the data for all three quantitative traits with ΔAIC >2.

606 Morph

Trait	Single rate model		Multiple rate model		ΔAIC
	AICc	AICweights	AICc	AICweights	
ED	253.9337	0.19991263	251.1600	0.800088	2.773681
sED	246.1558	0.004509138	235.3616	0.995491	10.794260
SL	538.3145	0.018806041	530.4053	0.981194	7.909184

607

608

609 **Table 2. Model averaged rate parameters for the measured traits in eye related morphs of**

610 ***Sinocyclocheilus.*** Normal-eyed and Micro-Eyed species indicate similar evolutionary rates with

611 marked shifts towards Blind species.

Trait	Model Averaged Rate		
	Blind	Micro-eyed	Normal-eyed
SL	45.3506	1597.9230	1275.5080
ED	11.3935	2.9984	3.8872
sED	24.9441	1.6925	2.2773

612

613

614

Fig.1

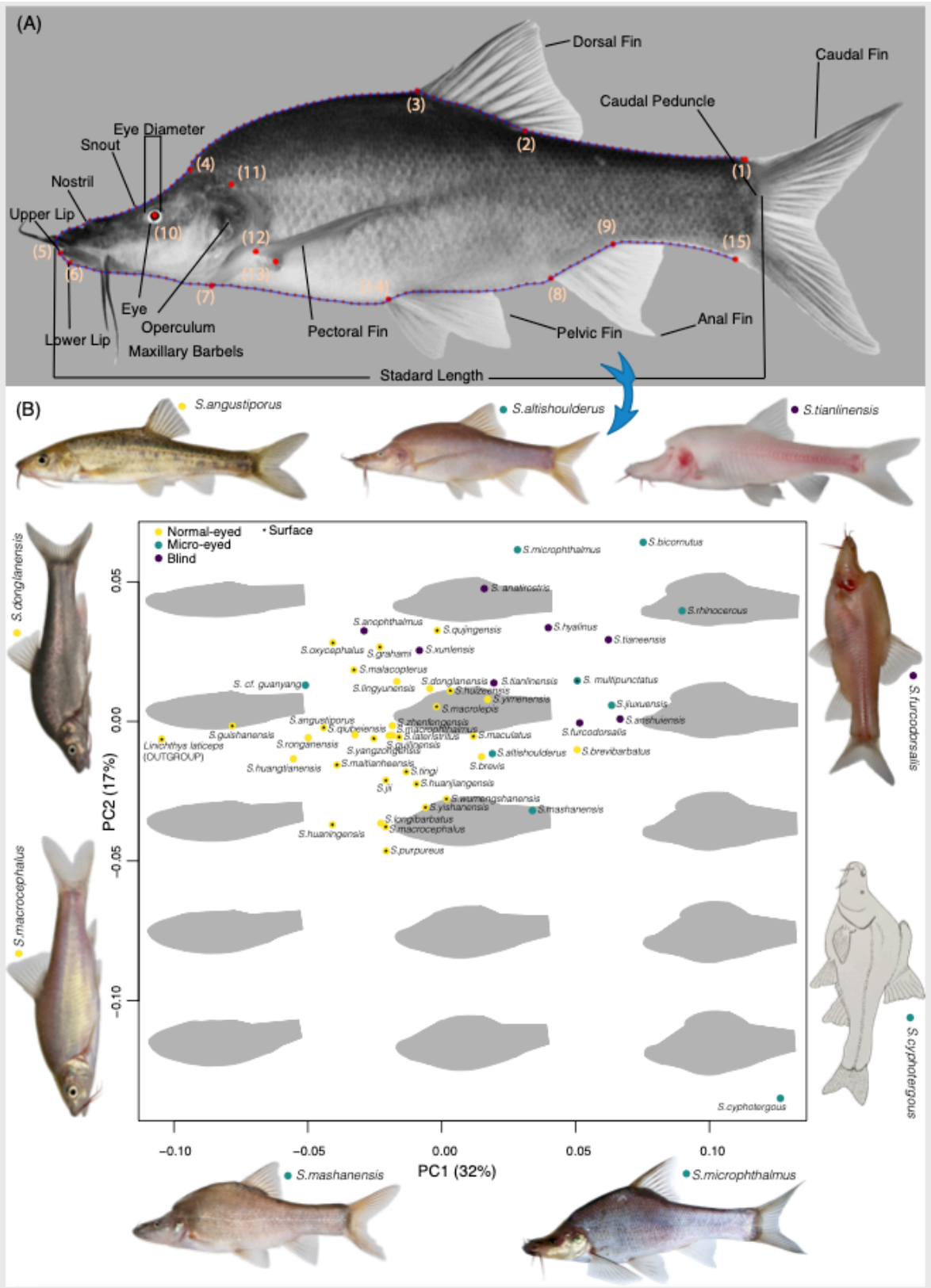
(A)
Dorsal Fin
Caudal Fin
Caudal Peduncle
Eye Diameter
Snout
Nostril
Upper Lip
Eye
Operculum
Maxillary Barbels
Lower Lip
Pectoral Fin
Pelvic Fin
Anal Fin
Stadard Length
(1)
(2)
(3)
(4)
(5)
(6)
(7)
(8)
(9)
(10)
(11)
(12)
(13)
(14)
(15)
(B)
S.angustiporus
S.altishoulderus
S.tianlinensis
S.donglanensis
S.macrocephalus
S.furcodorsalis
S.cyphotergous
S.mashanensis
S.microphthalmus
Normal-eyed
Micro-eyed
Blind
Surface
PC2 (17%)
PC1 (32%)
0.05
0.00
−0.05
−0.10
−0.10
−0.05
0.00
0.05
0.10

Fig.2.

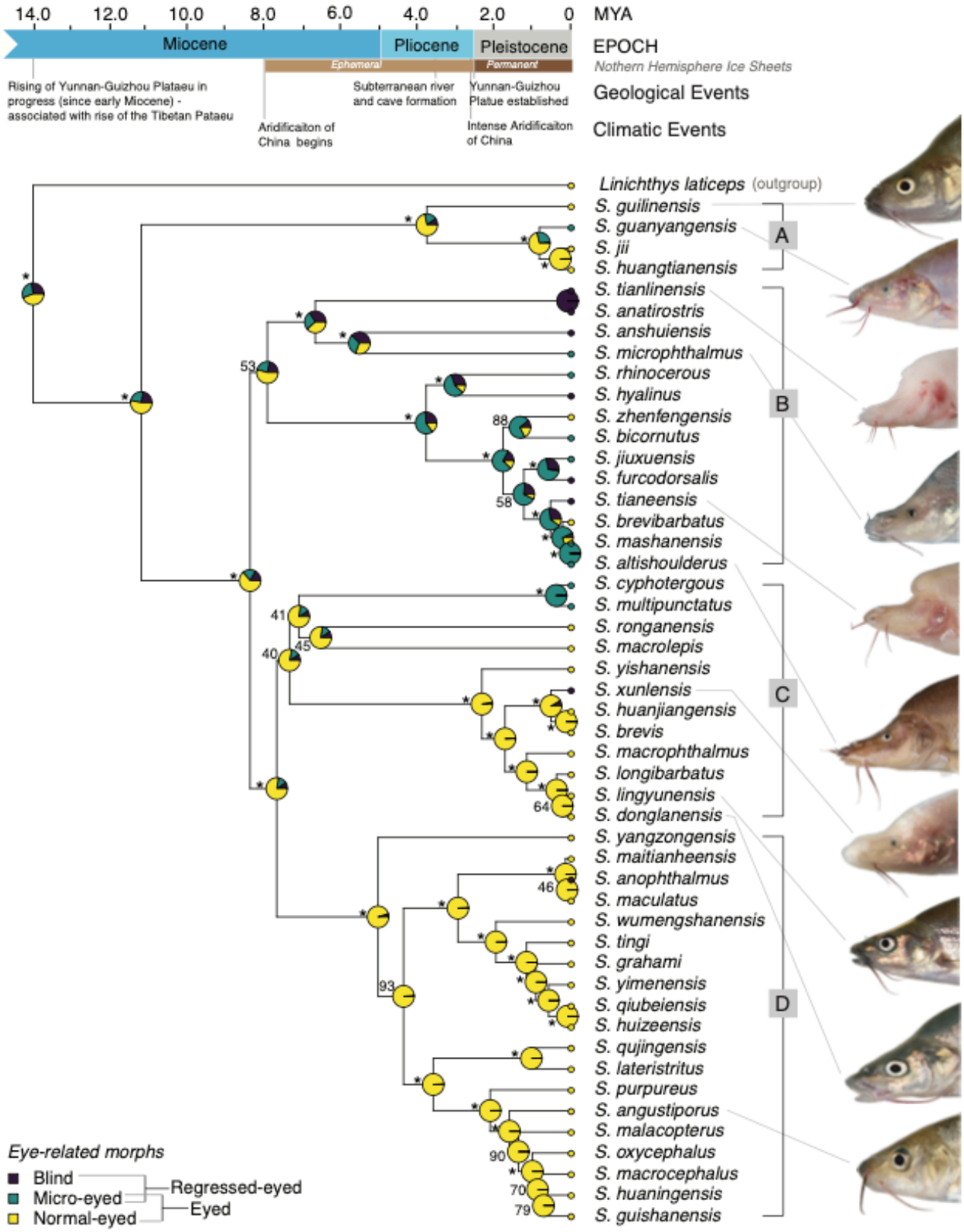
14.0
12.0
10.0
8.0
6.0
4.0
2.0
0
MYA
Miocene
Pliocene
Pleistocene
EPOCH
Ephemeral
Permanent
Nothern Hemisphere Ice Sheets
Rising of Yunnan-Guizhou Plataeu in progress (since early Miocene) - associated with rise of the Tibetan Pataeu
Aridificaiton of China begins
Subterranean river and cave formation
Yunnan-Guizhou Platue established
Intense Aridificaiton of China
Geological Events
Climatic Events
Linichthys laticeps (outgroup)
S. guilinensis
S. guanyangensis
S. jii
S. huangtianensis
S. tianlinensis
S. anatirostris
S. anshuiensis
S. microphthalmus
S. rhinocerous
S. hyalinus
S. zhenfengensis
S. bicornutus
S. jiuxuensis
S. furcodorsalis
S. tianeensis
S. brevibarbatus
S. mashanensis
S. altishoulderus
S. cyphotergous
S. multipunctatus
S. ronganensis
S. macrolepis
S. yishanensis
S. xunlensis
S. huanjiangensis
S. brevis
S. macrophthalmus
S. longibarbatus
S. lingyunensis
S. donglanensis
S. yangzongensis
S. maitianheensis
S. anophthalmus
S. maculatus
S. wumengshanensis
S. tingi
S. grahami
S. yimenensis
S. qiubeiensis
S. huizeensis
S. qujingensis
S. lateristritus
S. purpureus
S. angustiporus
S. malacopterus
S. oxycephalus
S. macrocephalus
S. huaningensis
S. guishanensis
A
B
C
D
53
88
58
41
45
40
64
46
93
90
70
79
Eye-related morphs
Blind
Micro-eyed
Normal-eyed
Regressed-eyed
Eyed

619

620 **Fig. 3.**

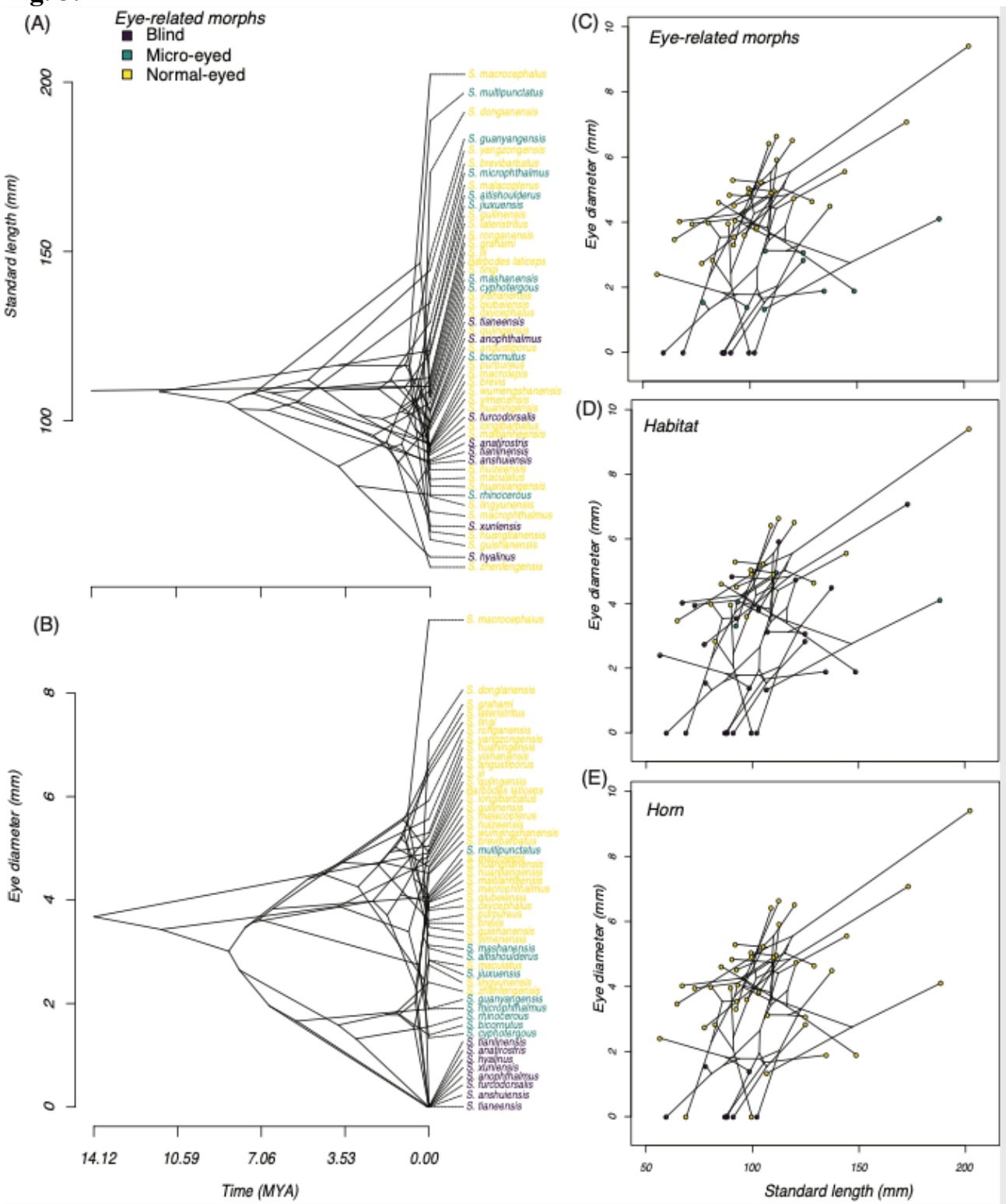

621

622

623

Fig.4.

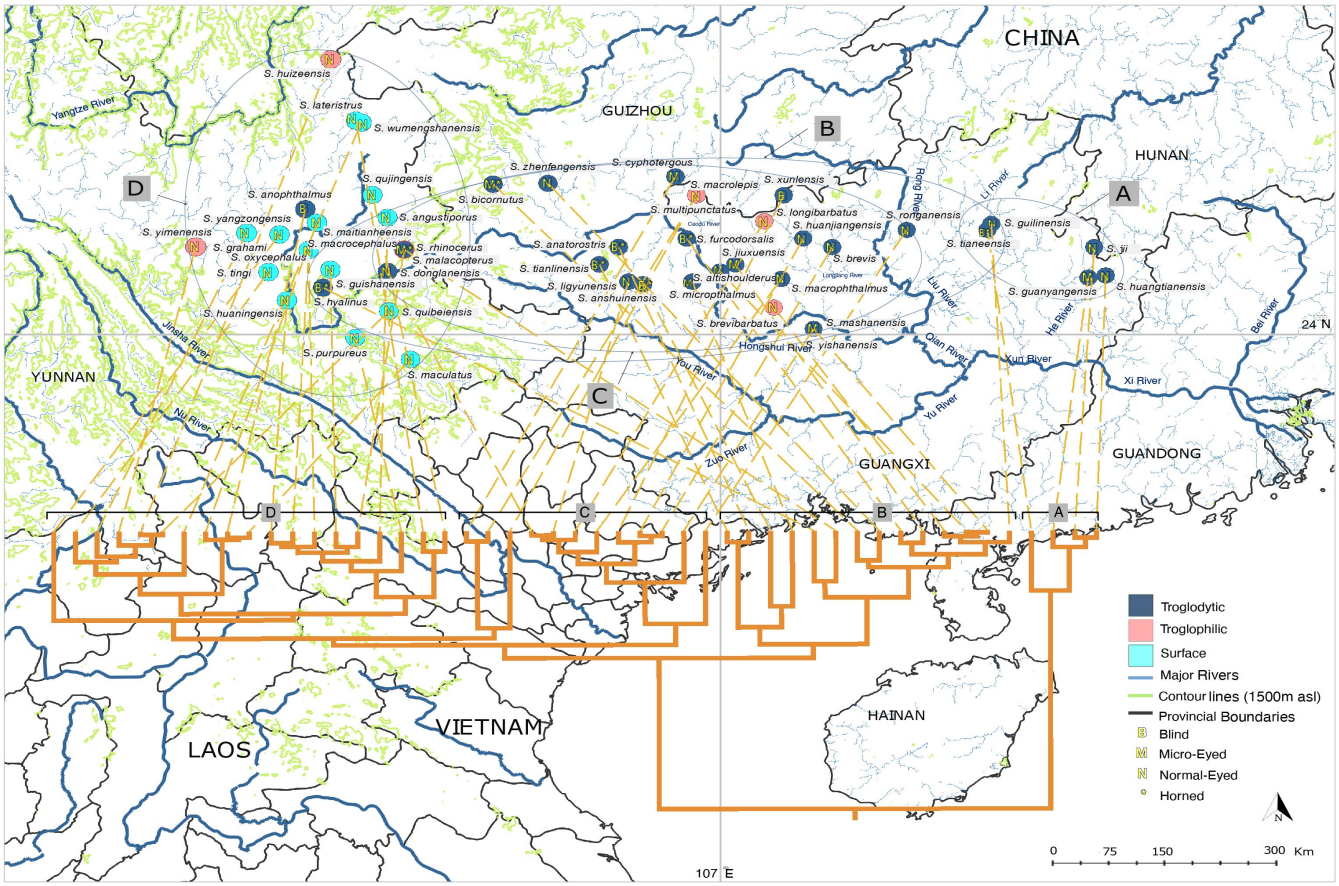
CHINA
GUIZHOU
HUNAN
YUNNAN
GUANGXI
GUANDONG
HAINAN
VIETNAM
LAOS
Yangtze River
Jinsha River
Nu River
You River
Zuo River
Hongshui River
Qian River
Yu River
Xun River
Xi River
He River
Bei River
Li River
Rong River
Liu River
24 N
107 E
A
B
C
D
S. huizeensis
S. lateristrus
S. wumengshanensis
S. qujingensis
S. anophthalmus
S. yangzongensis
S. yimenensis
S. grahami
S. oxycephalus
S. tingi
S. huaningensis
S. maitianheensis
S. macrocephalus
S. angustiporus
S. rhinocerus
S. malacopterus
S. donglanensis
S. guishanensis
S. hyalinus
S. quibeiensis
S. purpureus
S. maculatus
S. bicornutus
S. zhenfengensis
S. cyphotergous
S. anatorostris
S. tianlinensis
S. ligyunensis
S. anshuinensis
S. macrolepis
S. multipunctatus
S. furcodorsalis
S. jiuxuensis
S. altishoulderus
S. micropthalmus
S. brevibarbatus
S. xunlensis
S. longibarbatus
S. huanjiangensis
S. brevis
S. macrophthalmus
S. mashanensis
S. yishanensis
S. rongganensis
S. guilinensis
S. tianeensis
S. guanyangensis
S. huangtianensis
S. ji
Troglodytic
Troglophilic
Surface
Major Rivers
Contour lines (1500m asl)
Provincial Boundaries
Blind
Micro-Eyed
Normal-Eyed
Horned
0
75
150
300 Km

644

645 **Supplementary Information:**

646 Fig. S1. Maximum-likelihood reconstructions for the ancestral states of the habitat occupation

647 (Troglodytic, Troglophilic and Surface) on the phylogeny of the genus *Sinocyclocheilus*.

648

649 Fig. S2. Maximum-likelihood reconstructions for the ancestral state of the horn related trait

650 (presence/absence of horn) on the phylogeny of the genus *Sinocyclocheilus*.

651

652 Table S1. Species information and GenBank accession numbers of two mtDNA fragments

653 (*NADH4* and *cytb*) of 39 *Sinocyclocheilus* species. The information of the outgroup species

654 *Linichthys laticeps* (Cyprinidae) is also indicated along with calculated standard length (SL), eye

655 diameter (ED), standard eye diameter (sED), discrete trait categories related to eye morphology

656 (Blind, Micro-eyed, Normal eyed), presence or absence of a horn and habitat occupation

657 (Troglodytic, Troglophilic and surface) for all species used in the analysis. Accession numbers

658 indicated as XXXX will be accessible upon the acceptance of the manuscript.

Species name	SL	ED	SED	CYTB	NADH4	Morph	Habitat	Horn
Linichthys laticeps	110.20	4.91	4.45	AY854739	AY854796	Normal-eyed	Surface	Absent
S. altishoulderus	125.10±16.74	3.07±0.35	2.46	AY854724	AY854781	Micro-eyed	Troglodytic	Absent
S. anatirostris	88.40	0.00	0	AY854708	AY854765	Blind	Troglodytic	Present
S. angustiporus	99.57±19.79	5.05±0.77	5.07	AY854702	AY854759	Normal-eyed	Surface	Absent
S. anophthalmus	99.80	0.00	0	AY854715	AY854772	Blind	Troglodytic	Absent
S. anshuiensis	87.40	0.00	0	NC_027169	NC_039769	Blind	Troglodytic	Present
S. bicornutus	98.80	1.39	1.41	AY854730	AY854787	Micro-eyed	Troglodytic	Present
S. brevibarbatus	137.55±18.17	4.50±0.84	3.27	XXXX	-	Normal-eyed	Troglophilic	Absent

S. brevis	92.91±6.39	3.55±0.14	3.83	XXXX	-	Normal-eyed	Troglodytic	Absent
S. guanyangensis	148.92±7.39	1.90±1.14	1.27	AY854711	AY854768	Micro-eyed	Troglodytic	Absent
S. cyphotergous	106.95±13.08	1.34±0.61	1.25	AB196440	-	Micro-eyed	Troglodytic	Absent
S. donglanensis	173.37±15.94	7.09±0.69	4.09	AY854709	AY854766	Normal-eyed	Troglodytic	Absent
S. furcodorsalis	91.29±16.36	0.00	0	AY854694	AY854751	Blind	Troglodytic	Present
S. grahami	112.60	6.64	5.9	XXXX	-	Normal-eyed	Surface	Absent
S. guilinensis	120.68±15.04	4.74±0.33	3.93	XXXX	-	Normal-eyed	Troglodytic	Absent
S. guishanensis	64.90	3.48	5.35	AY854722	AY854779	Normal-eyed	Surface	Absent
S. huangtianensis	67.32±20.48	4.03±0.72	5.99	XXXX	-	Normal-eyed	Troglodytic	Absent
S. huaningensis	92.20	5.30	5.75	AY854718	AY854775	Normal-eyed	Surface	Absent
S. huanjiangensis	80.79±17.68	3.99±0.45	4.94	XXXX	-	Normal-eyed	Troglodytic	Absent
S. huizeensis	85.60	4.61	5.39	NC_044072	NC_039769	Normal-eyed	Troglophilic	Absent
S. hyalinus	59.80±28.43	0.00	0	AY854721	AY854778	Blind	Troglodytic	Present
S. jii	111.43±17.21	4.97±0.47	4.46	AY854727	AY854784	Normal-eyed	Troglodytic	Absent
S. jiuxuensis	125.10	2.84	2.27	AY854736	AY854793	Micro-eyed	Troglodytic	Absent
S. lateristritus	120.00	6.52	5.43	AY854703	AY854760	Normal-eyed	Surface	Absent
S. lingyunensis	77.69±9.35	2.75±0.60	3.53	AY854691	AY854748	Normal-eyed	Troglodytic	Absent
S. longibarbatus	90.63±1.82	4.84±0.24	5.34	AY854714	AY854771	Normal-eyed	Troglophilic	Absent
S. macrocephalus	202.30	9.42	4.65	AY854683	AY854740	Normal-eyed	Surface	Absent
S. macrolepis	93.30	4.06	4.35	AY854729	AY854786	Normal-eyed	Troglophilic	Absent
S. macrophthalmus	73.16±11.50	3.96±0.71	5.41	AY854735	AY854792	Normal-eyed	Troglodytic	Absent
S. maculatus	82.70	2.84	3.43	EU366193	EU366183	Normal-eyed	Surface	Absent

S. maitianheensis	90.00	3.96	4.4	AY854710	AY854767	Normal-eyed	Surface	Absent
S. malacopterus	129.20	4.65	3.6	AY854697	AY854754	Normal-eyed	Surface	Absent
S. mashanensis	107.36±5.72	3.13±0.34	2.91	XXXX	-	Micro-eyed	Troglodytic	Absent
S. microphthalmus	134.89±10.51	1.89±0.38	1.4	AY854687	AY854744	Micro-eyed	Troglodytic	Absent
S. multipunctatus	188.60	4.11	2.18	AY854712	AY854769	Micro-eyed	Troglophilic	Absent
S. oxycephalus	103.10	3.80	3.69	AY854685	AY854742	Normal-eyed	Surface	Absent
S. purpureus	97.60	3.61	3.7	EU366194	EU366177	Normal-eyed	Surface	Absent
S. qiubeiensis	103.30	3.84	3.72	EU366195	EU366181	Normal-eyed	Surface	Absent
S. qujingensis	99.90	4.91	4.92	AY854719	AY854776	Normal-eyed	Surface	Absent
S. rhinocerous	78.20	1.55	1.98	AY854720	AY854777	Micro-eyed	Troglodytic	Present
S. ronganensis	112.72	5.92	5.25	NC_032385	NC_039769	Normal-eyed	Troglodytic	Absent
S. tianeensis	102.34±12.43	0.00	0	AY854717	AY854774	Blind	Troglodytic	Present
S. tianlinensis	87.96±27.97	0.00	0	XXXX	-	Blind	Troglodytic	Present
S. tingi	109.00	6.42	5.89	AY854701	AY854758	Normal-eyed	Surface	Absent
S. wumengshanensis	92.80	4.52	4.87	NC_039769	NC_039769	Normal-eyed	Surface	Absent
S. xunlensis	69.01±21.44	0.00	0	EU366187	EU366184	Blind	Troglodytic	Absent
S. yangzongensis	144.50	5.56	3.85	AY854725	AY854782	Normal-eyed	Surface	Absent
S. yimenensis	92.50	3.31	3.58	EU366192	EU366179	Normal-eyed	Troglophilic	Absent
S. yishanensis	105.34±8.15	5.23±0.23	4.97	XXXX	-	Normal-eyed	Troglodytic	Absent
S. zhenfengensis	56.78	2.41	4.24	MK610342	MK610347	Normal-eyed	Troglodytic	Absent

Table S2. Information of digitized images used in the morphometric geometric analysis. Table indicates the voucher number of the specimen used for the analysis and the reference from which the image was obtained. Images photographed during the current study are also indicated with voucher numbers stated as GXUXXX (GXU: Guangxi University, China).

Species name	Reference	Voucher #
Linichthys laticeps	Zhang, E., and F. Fang. 2005. Linichthys: A New Genus of Chinese Cyprinid Fishes (Teleostei: Cypriniformes). Copeia 2005:61–67.	*IHB 78X6242*
S. altishoulderus	Guangxi University (this study).	*GXU001, GXU002, GXU003*
S. anatirostris	Romero, A., Y. Zhao, and X. Chen. 2009. The Hypogean fishes of China. Environ Biol Fish 86:211–278.	*IHB 84VII255,*
S. angustiporus	Guangxi University (this study).	*GXU007, GXU008 , GXU009*
S. anophthalmus	Romero, A., Y. Zhao, and X. Chen. 2009. The Hypogean fishes of China. Environ Biol Fish 86:211–278.	*KIZ 865949*
S. anshuiensis	Xi, G., W. Tie-Jun, W. Mu-Lan, and Y. Jian. 2013. A new blind barbine species, *Sinocyclocheilus anshuiensis* sp. nov.(Cypriniformes: Cyprinidae) from Guangxi, China. Kunming Institute of Zoology, Chinese Academy of Sciences.	*12070276*
S. bicornutus	Romero, A., Y. Zhao, and X. Chen. 2009. The Hypogean fishes of China. Environ Biol Fish 86:211–278.	*IHB 12209043-9o5o241*
S. brevibarbatus	Guangxi University (this study).	*GXU010, GXU011, GXU012*
S. brevis	Guangxi University (this study).	*GXU013,*

	Romero, A., Y. Zhao, and X. Chen. 2009. The Hypogean fishes of China. Environ Biol Fish 86:211–278.	*GXU014* *IHB12209033-87087496*
S. cyphotergous	Romero, A., Y. Zhao, and X. Chen. 2009. The Hypogean fishes of China. Environ Biol Fish 86:211–278. Huang, J., A. Gluesenkamp, D. Fenolio, Z. Wu, and Y. Zhao. 2017. Neotype designation and redescription of *Sinocyclocheilus cyphotergous* (Dai) 1988, a rare and bizarre cavefish species distributed in China (Cypriniformes: Cyprinidae). Environ Biol Fish 100:1483–1488.	*IHB 12209040* *ASIZB 204678*
S. donglanensis	Guangxi University (this study).	*GXU015, GXU016, GXU017*
S. furcodorsalis	Guangxi University (this study).	*GXU018, GXU019, GXU020*
S. grahami	Romero, A., Y. Zhao, and X. Chen. 2009. The Hypogean fishes of China. Environ Biol Fish 86:211–278.	*ASIZB 03496*
S. guanyangensis	Guangxi University (this study).	*GXU004,GXU005, GXU006*
S. guilinensis	Guangxi University (this study).	*GXU021, GXU022, GXU023*
S. guishanensis	Romero, A., Y. Zhao, and X. Chen. 2009. The Hypogean	*Li980514005*

	fishes of China. Environ Biol Fish 86:211–278.	
S. huangtianensis	Guangxi University (this study).	*GXU024, GXU025, GXU026*
S. huaningensis	Romero, A., Y. Zhao, and X. Chen. 2009. The Hypogean fishes of China. Environ Biol Fish 86:211–278.	*ASIZB79228*
S. huanjiangensis	Guangxi University (this study).	*GXU027, GXU028, GXU029*
S. huizeensis	Cheng, C., P. Xiao-Fu, C. Xiaoyong, J. Li, L. Ma, and J. Yang. 2015. A new species of the genus *Sinocyclocheilus*(Teleostei:Cypriniformes), from Jinshajiang Drainage, Yunnan, China. Cave Research 1:1–4.	*KIZ2013001246*
S. hyalinus	Romero, A., Y. Zhao, and X. Chen. 2009. The Hypogean fishes of China. Environ Biol Fish 86:211–278. You, H., C. Xiaoyong, X. Ti-Qao, and Y. Jun-Xing. 2013. Three-dimensional morphology of the *Sinocyclocheilus hyalinus* (Cypriniformes : Cyprinidae) horn based on synchrotron X-ray microtomography. Zoological research 34:128–134.	*KIZ916001* *Photograph in life*
S. jii	Romero, A., Y. Zhao, and X. Chen. 2009. The Hypogean fishes of China. Environ Biol Fish 86:211–278.	*ASIZB62726*

	Baradi, W., Z. Yahui, Z. Chunguang, D. Rongji, and A. Abdul. 2013. Anatomical Studies of the Olfactory Epithelium of Two Cave Fishes *Sinocyclocheilus jii* and *S. furcodorsalis* (Cypriniformes: Cyprinidae) from China. Pakistan Journal of Zoology 45:1091 –1101.	*Photograph in life*
S. jiuxuensis	Romero, A., Y. Zhao, and X. Chen. 2009. The Hypogean fishes of China. Environ Biol Fish 86:211–278.	*ASIZB102260*
S. lateristritus	Romero, A., Y. Zhao, and X. Chen. 2009. The Hypogean fishes of China. Environ Biol Fish 86:211–278.	*IHB12209036-865027*
S. lingyunensis	Guangxi University (this study). Romero, A., Y. Zhao, and X. Chen. 2009. The Hypogean fishes of China. Environ Biol Fish 86:211–278.	*GXU030* *ASIZB 73038*
S. longibarbatus	Guangxi University (this study).	*GXU031, GXU032, GXU033*
S. macrocephalus	Romero, A., Y. Zhao, and X. Chen. 2009. The Hypogean fishes of China. Environ Biol Fish 86:211–278.	*IHB12209012-662001*
S. macrolepis	Romero, A., Y. Zhao, and X. Chen. 2009. The Hypogean fishes of China. Environ Biol Fish 86:211–278.	*IHB12209035-87IV457*
S. macrophthalmus	Guangxi University (this study).	*GXU034,GXU035,GXU036*
S. maculatus	Romero, A., Y. Zhao, and X. Chen. 2009. The Hypogean fishes of China. Environ Biol Fish 86:211–278.	*Li870808001*
S. maitianheensis	Romero, A., Y. Zhao, and X. Chen. 2009. The Hypogean fishes of China. Environ Biol Fish 86:211–278.	*IHB12209039-874001*
S. malacopterus	Romero, A., Y. Zhao, and X. Chen. 2009. The Hypogean	*KIZ775831*

	fishes of China. Environ Biol Fish 86:211–278.	
S. mashanensis	Guangxi University (this study).	*GXU037, GXU038, GXU039*
S. microphthalmus	Guangxi University (this study).	*GXU040, GXU041, GXU042*
S. multipunctatus	Romero, A., Y. Zhao, and X. Chen. 2009. The Hypogean fishes of China. Environ Biol Fish 86:211–278.	*ASIZB73000*
S. oxycephalus	Romero, A., Y. Zhao, and X. Chen. 2009. The Hypogean fishes of China. Environ Biol Fish 86:211–278.	*IHB12209013-652047*
S. purpureus	Romero, A., Y. Zhao, and X. Chen. 2009. The Hypogean fishes of China. Environ Biol Fish 86:211–278.	*IHB12209015-731004*
S. qiubeiensis	Romero, A., Y. Zhao, and X. Chen. 2009. The Hypogean fishes of China. Environ Biol Fish 86:211–278.	*Li990527002*
S. qujingensis	Romero, A., Y. Zhao, and X. Chen. 2009. The Hypogean fishes of China. Environ Biol Fish 86:211–278.	*ASIZB78790*
S. rhinocerous	Romero, A., Y. Zhao, and X. Chen. 2009. The Hypogean fishes of China. Environ Biol Fish 86:211–278.	*ASIZB93907*
S. ronganensis	FuGuang, L., H. Jie, L. Xia, L. Tong, and W. YanHong. 2016. *Sinocyclocheilus ronganensis* Luo, Huang et Wen sp. nov., a new species belonging to *Sinocyclocheilus* Fang from Guangxi (Cypriniformes: Cyprinidae). Guangxi Academy of Agricultural Sciences 47:650–655.	*20151114001*
S. tianeensis	Guangxi University (this study).	*GXU043, GXU044, GXU045*

S. tianlinensis	Guangxi University (this study).	*GXU052, GXU053, GXU054*
S. tingi	Romero, A., Y. Zhao, and X. Chen. 2009. The Hypogean fishes of China. Environ Biol Fish 86:211–278.	*ASIZB60227*
S. wumengshanensis	Romero, A., Y. Zhao, and X. Chen. 2009. The Hypogean fishes of China. Environ Biol Fish 86:211–278.	*KIZ82100006*
S. xunlensis	Guangxi University (this study).	*GXU046, GXU047, GXU048*
S. yangzongensis	Romero, A., Y. Zhao, and X. Chen. 2009. The Hypogean fishes of China. Environ Biol Fish 86:211–278.	*KIZ6351069*
S. yimenensis	Romero, A., Y. Zhao, and X. Chen. 2009. The Hypogean fishes of China. Environ Biol Fish 86:211–278.	*Li030509009*
S. yishanensis	Romero, A., Y. Zhao, and X. Chen. 2009. The Hypogean fishes of China. Environ Biol Fish 86:211–278.	*GXU049, GXU050, GXU051*
S. zhenfengensis	Liu, T., H. Q. Deng, L. Ma, N. Xiao, and J. Zhou. 2018. *Sinocyclocheilus zhenfengensis* , a new cyprinid species (Pisces: Teleostei) from Guizhou Province, Southwest China. J Appl Ichthyol 34:945–953.	*GZNU20120701001*

Table S3. Calculated Principal Component values (PC1, PC2 and PC3) of all the specimens used in the current analysis

Spname	PC1val	PC2val	PC3cal
Linichthys laticeps	0.1069618	-0.006044939	-0.032010383
S. altishoulderus	-0.01804998	-0.010081536	-0.046423134

S. anatirostris	-0.01766386	0.046175863	0.051169448
S. angustiporus	0.04334953	-0.002675304	0.034186136
S. anophthalmus	0.02908059	0.031606384	0.00917709
S. anshuiensis	-0.06639039	-0.000250595	-0.004873197
S. bicornutus	-0.07667729	0.060886565	0.012973894
S. brevibarbatus	-0.05048176	-0.011045867	0.006805293
S. brevis	-0.0142754	-0.011768784	-0.001763996
S. guanyangensis	-4.38E-05	0.015156895	-0.025200906
S. cyphotergous	-0.1220022	-0.139796596	0.008525168
S. donglanensis	0.004198408	0.013428914	-0.021746042
S. furcodorsalis	-0.050741	-0.000898602	-0.044412032
S. grahami	0.02231859	0.026236004	0.022098623
S. guilinensis	0.01963493	-0.0033727	-0.023009295
S. guishanensis	0.07886827	0.00257981	-0.059167855
S. huangtianensis	0.05562456	-0.011114954	0.021111628
S. huaningensis	0.04117411	-0.037450418	0.031061221
S. huanjiangensis	0.009958768	-0.021868616	0.007063138
S. huizeensis	-0.003779219	0.010286192	0.031012201
S. hyalinus	-0.03974731	0.030183657	0.039671171
S. jii	0.02155773	-0.019701057	-0.005284772
S. jiuxuensis	-0.06337799	0.004932247	-0.008080491
S. lateristritus	0.01609448	-0.006156199	0.021918263
S. lingyunensis	0.01666848	0.015544267	0.002003128
S. longibarbatus	0.0238826	-0.037134912	0.007645544
S. macrocephalus	0.0223646	-0.03930768	0.034945546
S. macrolepis	0.002586613	0.0056233	-0.005281302

S. macrophthalmus	0.01921085	-0.004423179	0.011957836
S. maculatus	-0.01164108	-0.003338214	-0.043022304
S. maitianheensis	0.04058493	-0.015399253	-0.004022456
S. malacopterus	0.03369873	0.016341474	0.002649988
S. mashanensis	-0.03299028	-0.033529198	-0.005547116
S. microphthalmus	-0.02936266	0.061223556	-0.040563771
S. multipunctatus	-0.05126049	0.014657848	-0.010821531
S. oxycephalus	0.04140438	0.030989746	-0.036348165
S. purpureus	0.02288238	-0.045035385	-0.018448807
S. qiubeiensis	0.03248934	-0.003880679	0.012191068
S. qujingensis	0.000644406	0.033555511	0.046291334
S. rhinocerous	-0.08985807	0.03649387	-0.020510521
S. ronganensis	0.05067357	-0.004282673	-0.02013066
S. tianeensis	-0.06234116	0.02827463	-0.030564848
S. tianlinensis	-0.01905521	0.012948686	-0.00406653
S. tingi	0.01508119	-0.019031787	-0.002178747
S. wumengshanensis	-0.000171791	-0.027155405	0.003238896
S. xunlensis	0.008420042	0.022462118	0.047598226
S. yangzongensis	0.02622031	-0.003887167	-0.006000758
S. yimenensis	-0.01762049	0.008265106	0.019258774
S. yishanensis	0.007505367	-0.029610044	-0.01952727
S. zhenfengensis	0.01938822	-0.002301361	0.003044235

673 **Fig.S1.**

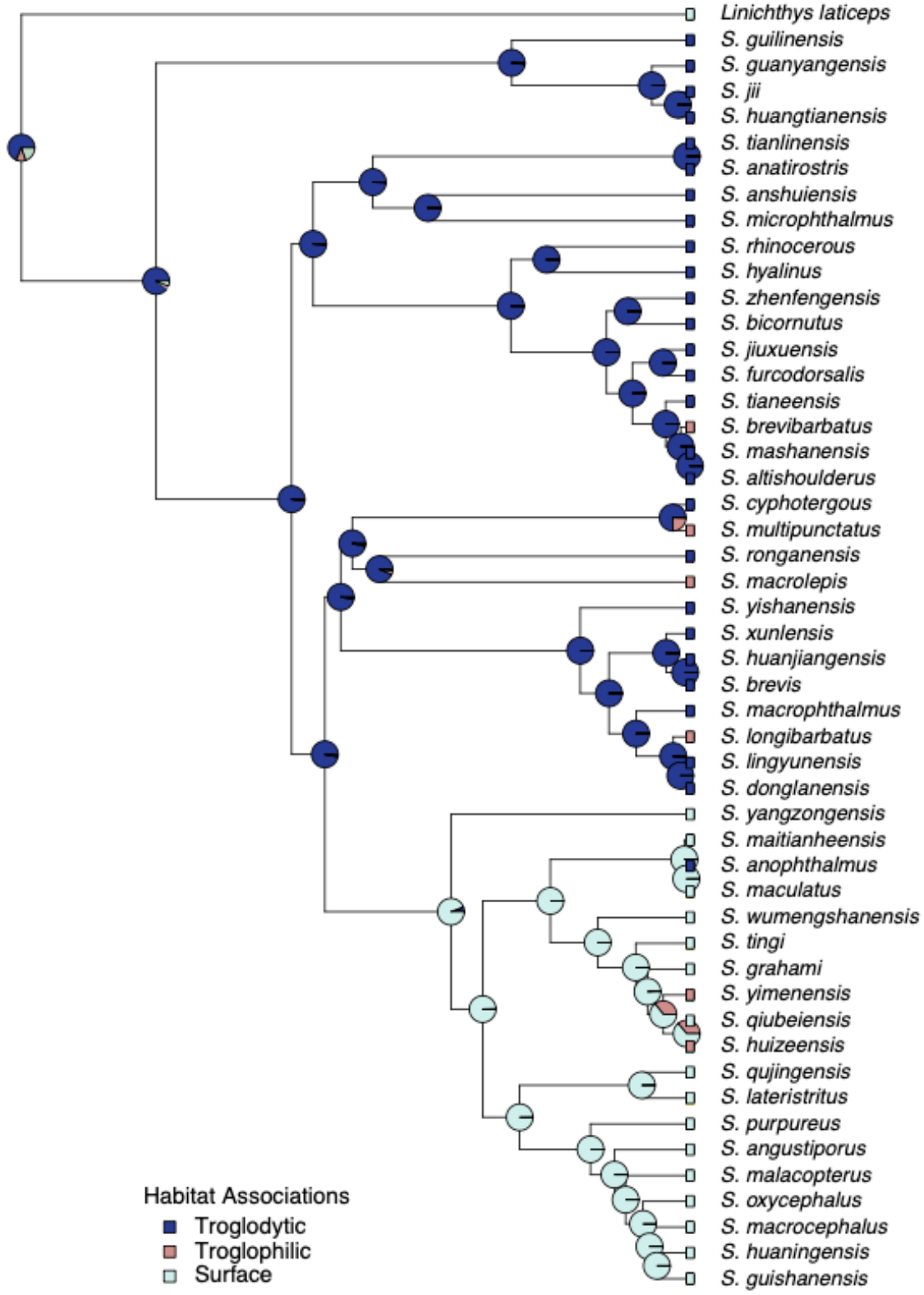

674
675

676 **Fig.S2.**

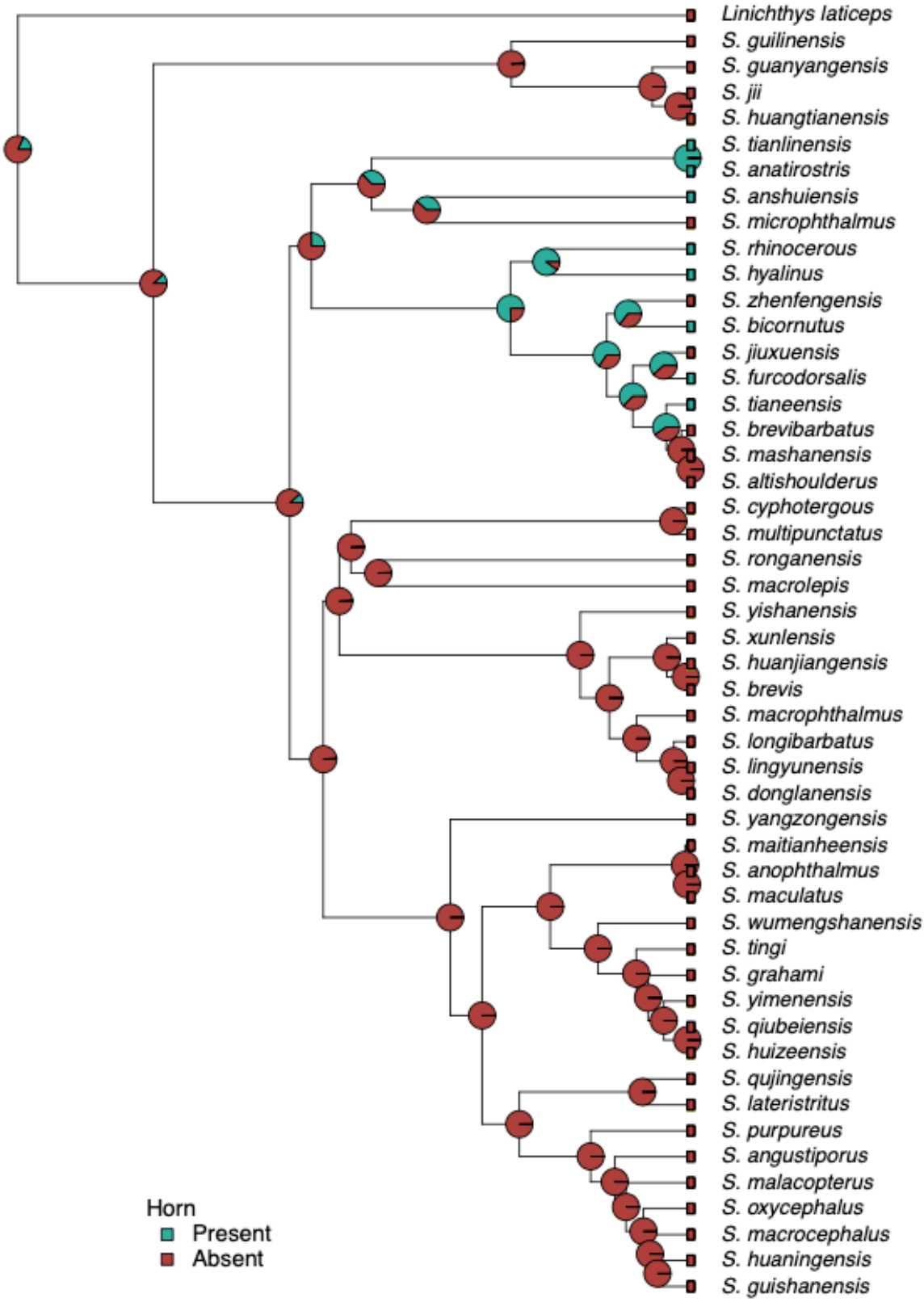

677